Technical

Report

Final Report
F-B2299

SPACE AND RELATED BIOLOGICAL AND INSTRUMENTATION STUDIES

by
R. J. Gibson
R. M. Goodman

FINAL REPORT
March 1970 - November 1971

Prepared for
NATIONAL AERONAUTICS AND SPACE ADMINISTRATION
Contract NSR-039-005-018

THE FRANKLIN INSTITUTE RESEARCH LABORATORIES
BENJAMIN FRANKLIN PARKWAY • PHILADELPHIA, PENNA. 1910

Technical

Final Report
F-B2299

Report

SPACE AND RELATED BIOLOGICAL
AND
INSTRUMENTATION STUDIES

by
R. J. Gibson
R. M. Goodman

FINAL REPORT
March 1970 - November 1971

Prepared for
NATIONAL AERONAUTICS AND SPACE ADMINISTRATION
Contract NSR-039-005-018

THE FRANKLIN INSTITUTE RESEARCH LABORATORIES
BENJAMIN FRANKLIN PARKWAY • PHILADELPHIA, PENNA. 19103

ACKNOWLEDGEMENTS

The authors acknowledge contributions to the work reported herein of Mr. John DeBenedictis, Mr. John Price, Mr. Richard Field* and Mr. Richard Quinn.

*Deceased.

TABLE OF CONTENTS

LIST OF FIGURES

LIST OF FIGURES (Cont'd)

1.0 INTRODUCTION

Research and experimental effort was carried out on high-density photo-optical recorder design, implantable pH electrodes and the magnetic/doppler blood-flow sensor.

The recorder design approach was evolved for potential application in biologic and ecologic studies.

The pH electrode effort was a modest continuation of our attack on the extremely difficult problem of evolving such electrodes which are implantable in a physiologically acceptable way and which will retain their accuracy and stability for time periods sufficiently long as to permit chronic studies.

Our work with the magnetic/doppler blood-flow sensor represented preliminary efforts toward proving the practical feasibility of the theoretical approach.

We believe our initial efforts to be of considerable value to the subsequent work which yet remains to be prosecuted.

1.1 Transducers

Within our limited funding, work was continued on the development of the pH electrode and initial circuit designs to prove the feasibility of the combined principle magnetic/doppler flowmeter.

1.2 pH Electrode Development

A very limited effort was carried out in this period due to effort required in other phases of the work. Measurements were made of the series "H" electrodes after being stored at ambient conditions for over six months. The results were not particularly encouraging after the initially promising results reported for the "H" series in report A-B2299-5. These electrodes, for an extended period after fabrication, showed uniformity and little change. The most recent measurements, however, showed all H-electrodes potentials increasing by an average of about 50 millivolts. This increase was not uniform, however, with H_1 increasing the greatest amount and H_2 and H_3 increasing by approximately the same amount, but less than H_1. The change was far greater than could be expected due to surface changes of the metal surface itself or due to contamination of the surface. Another cause of change was looked for. A careful microscopic examination of the electrode surfaces revealed a number of hairline cracks in the rhodium plating. In some cases these cracks showed a distinct discoloration along their path. A crack in the plating which would expose the base metal (silver) would completely explain the change in potential and the differences between the electrodes. There are a number of possible solutions to the cracking problem, among these are: annealing of plating and substrate after plating, burnishing of each of several plating layers, thinner plating film, and a change in plating schedule. The fact that the cracks did not occur until after six months is encouraging in that it shows that the stresses were small. It is

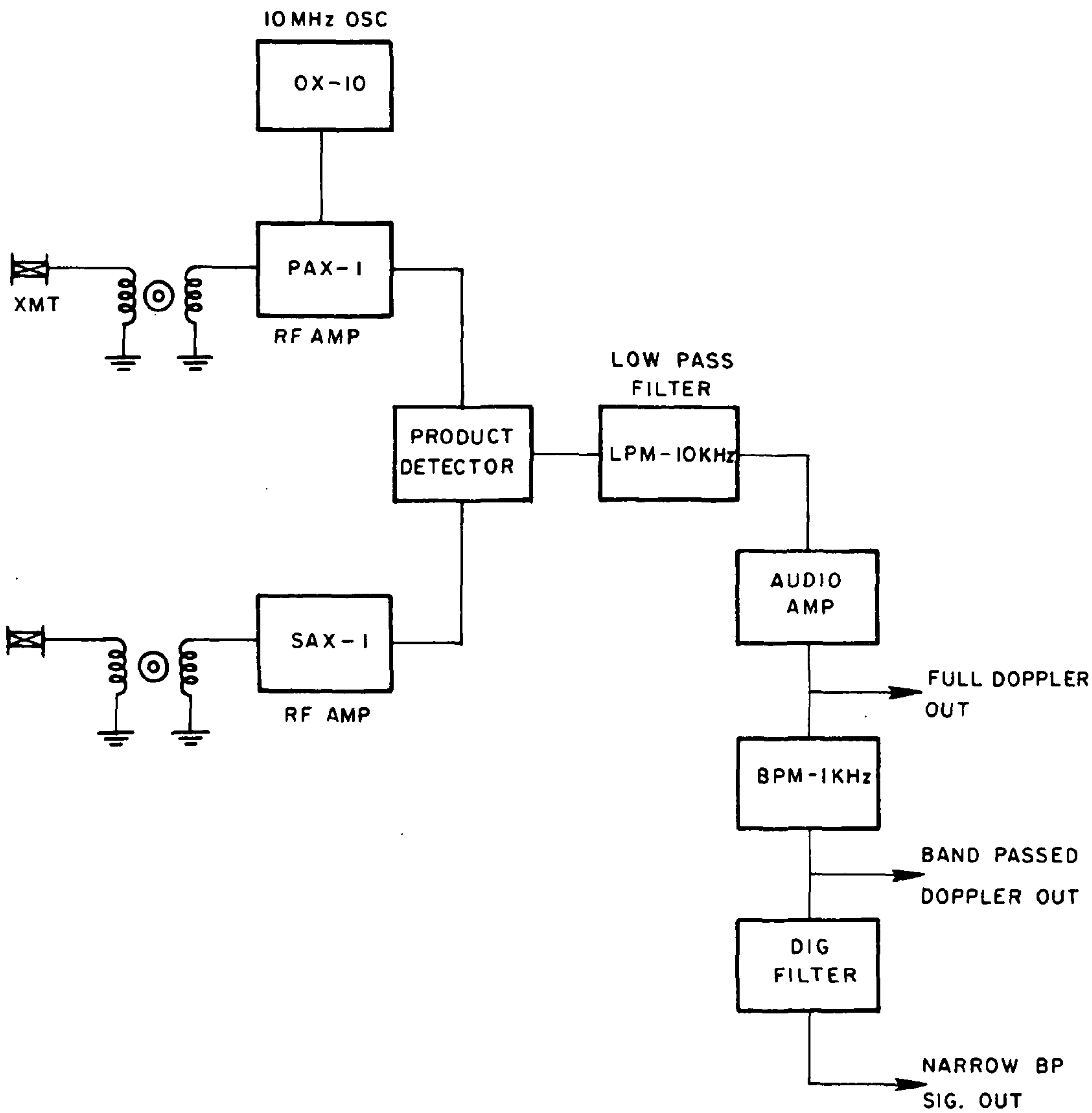

Fig. 1.3-1. Block Diagram of Doppler Pulse Output Circuit

discouraging in that it will be difficult to assess a change in results due to a change in technique in a reasonably short time. The process of fabrication which we have evolved in this development will produce pH electrodes which are uniform, consistent and similar and which yield a sufficiently high slope of millivolts per pH to be successfully used with implantable telemeters. Their present life-time is apparently limited (to something less than six months) by internal stresses in the rhodium plating. This failure mode is sufficiently large in electrode potential change however to be obvious when it occurs.

We look forward to further improvement in our fabrication techniques and to continuous evaluation of performance with time. We hope to evaluate iridium plating versus our present rhodium technique. Further, we would plan to consider protective, but permeable electrode coatings which are long-lived and physiologically acceptable.

1.3 Magnetic/Doppler Flow Sensor Development

A complete description of the general theory of operation of this combined principle flowmeter is given in the (1) annual report A-B2299-5. At that time only the system aspects of the approach were considered. In this report specific implementation of some of the system components are described. A block diagram of the circuits are shown in Figure 1.3-1.

Preliminary component selection and some specific calculations were described in (2) Q-B2299-24. Since that time some changes have been made and the following circuits were built and tested.

Oscillator circuit (10 MHz): Because of the ease of circuit construction for breadboard testing, the International Oscillator Kit OX-LO (3) was used. This is a single transistor crystal controlled oscillator producing a good output. It was assembled on a 1" x 1" printed circuit board. The circuit, components and operating specifications are shown in Figure 1.3-2. This oscillator was built and tested and performed extremely well meeting specifications as tested.

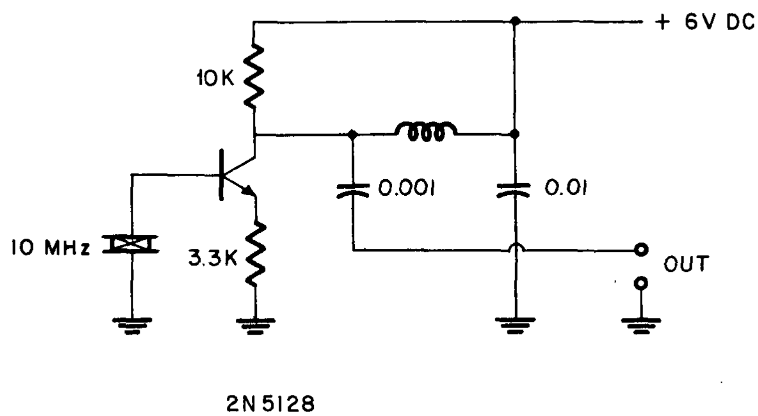

Specifications

RF out - 0.2 VRMS into 50 ohms
DC supply 6-9 volts
Freq tol. with ex crystal, .02%
Freq change with 1 volt supply change - .001% max
Output level change with 1 volt sup. change ≈ 2 db

Figure 1.3-2. Ten Megahertz Oscillator

The oscillator must be followed by an RF power amplifier providing sufficient power to actuate the crystal transducer for ultrasonic projection. For this purpose the International RF power amplifier PAX-1 was chosen (4). This amplifier will provide up to 200 milliwatts of fairly pure sine-wave power into a 50 ohm load. (Ten megaherz Barium Zirconate-Titanate crystal material cut to a projection area of 0.1" x 0.3" will have approximately 50 ohms impedance operating into water or tissue.) The power amplifier is constructed on a 1" x 1" square printed circuit. The circuit and specification are shown in Figure 1.3-3. The power amplifier was constructed and no difficulty was encountered in matching the output to a 50 ohm load. The output was found to be as desired and should provide sufficient power to activate the transmitter crystal.

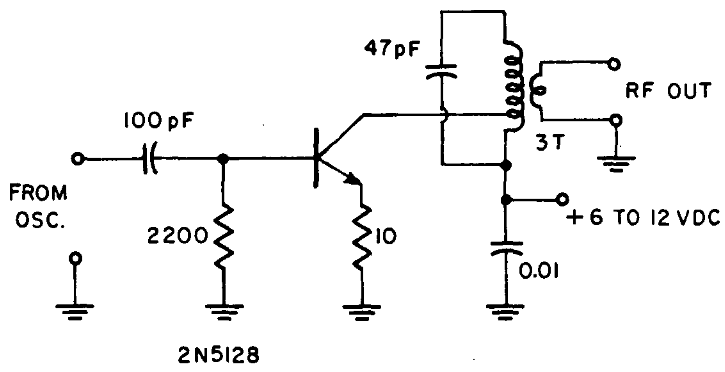

Specifications

Output - 30 to 200 MW
Output - Low imped. link ≈ 50 ohms
Harmonics - Less than 20 db

Figure 1.3-3 RF Power Amplifier

For the receiving sections of the circuit a very high gain is required. The received signal from a blood vessel in tissue has been estimated to be at least 70 db to 80 db (2A) down from the transmitted signal in a configuration similar to that proposed here. A simple calculation is given below.

$$P\ (\text{recv'd}) = 10^{-7} \text{ to } 10^{-8}\ P(\text{trans.})$$

$$P\ (\text{recv'd}) = 200 \text{ milliwatts} \times 10^{-7} \text{ or } 10^{-8}$$

$$= 20 \text{ to } 2\ \mu\text{watts}$$

$$\text{Recv'd power} \simeq 2 \text{ to } 20\ \mu\text{watts}$$

Into a 50 ohm receiver crystal this would provide:

$$P\ (\text{recv'd}) = \frac{E^2}{R};\ R = 50 \text{ ohm}$$

$$E^2 = PR$$

$$= 2 \text{ to } 20 \times 10^{-6} \times 50$$

$$= 100 \text{ to } 1000\ (\text{microvolts})^2$$

and $E = 10 \text{ to } 30\ \mu\text{volts received.}$

For the product detector described later, a 3μV signal is required for a 10 db (s+n)/n at the audio output and 9μV for 20 db (s+n)/n is required. It was therefore considered wise to provide some signal gain and matching before applying the signal to the product detector. For this purpose an International SAX-1 small signal RF amplifier[5] was chosen. This unit was constructed on a 1" x 1" printed circuit board and will provide a gain of about 10 db to 15 db (or 3 to 5 in voltage gain) at 10 MHz which should just be sufficient to produce a good signal-to-noise ratio at the detector output. The circuit and specifications are shown in Figure 1.3-4. This circuit performs well at very low input signals. With a 500 ohm resistor in place of the output link, a voltage gain of 15 was measured at 10 MHz, from less than 50 microvolts in up to 50 millivolts in. Above 50 millivolts second harmonic distortion increased until at about 100 millivolts in, the distortion was considered bad. Measurements were difficult to make below 50 microvolts although indications were that the gain held up to well below 10 microvolts. It appears that this amplifier will perform well as the input stage for this circuit.

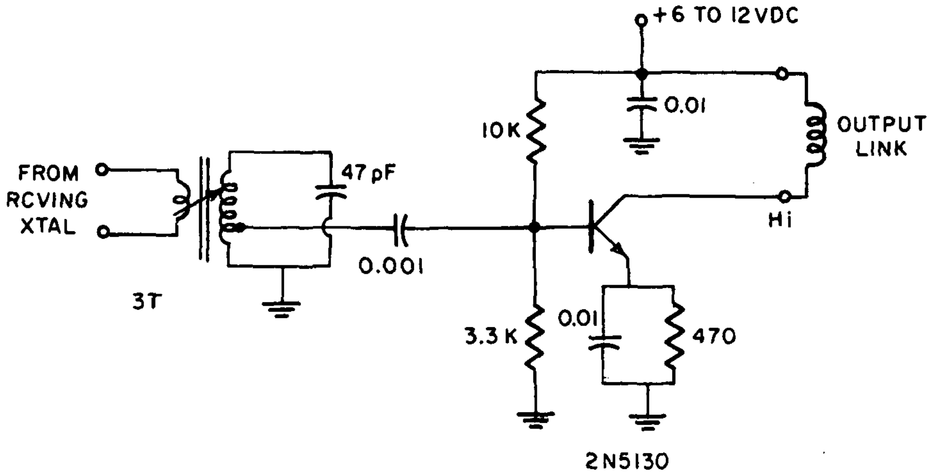

FREQ - with 47 pF 8-13 MHz tune with slug
GAIN - 15 db @ 3 MHz; 10 db @ 150 MHz
SENS - Useful to 1 μV
INPUT & OUTPUT - Low Imp Links

Figure 1.3-4. Small Signal RF Amplifier

The signal from this amplifier will then be inserted into the signal port of the product detector. A portion of the carrier from the RF power amplifier will be limited with diodes to form approximately a 300 millvolt square wave which will inserted into the carrier port of the product detector.

The Motorola integrated circuit[6] balanced modulator detector MC 1596G is uniquely suited for this application. It is an integrated circuit consisting of 8 transistors, 1 diode and three resistors in a 602A case (about To-5 size can with 10 leads).

This unit was designed to produce an output voltage which is the product of an input signal and a switching function (carrier). A product multiplier circuit is discussed: This circuit is really an rf mixer circuit with an audio output. The audio output signal is the difference between the signal frequency and the carrier frequency. The MC1596G in this configuration suppresses both rf frequencies leaving only the desired audio frequency output. This is precisely what is required of a doppler signal demodulator since the carrier is doppler shifted from 0 to about 12 KHz by blood flow; the frequency shift being proportional to the fluid flow *velocity*. A modification of this circuit for higher sensitivity and a single voltage supply[7] is shown in Figure 1.3-5. This is an extremely sensitive circuit having a dynamic range of over 90 db, being useful for input signal voltages from 3 microvolts to 100 millivolts without significant distortion. At 3 microvolts in, a signal-to-noise ratio of 10 db is realized with 9 microvolts giving 20 db (s+n)/n. The resistor from pins 2 and 3 may be used for effecting a compromise between gain and input signal handling capacity. A low-pass filter connected to pin 9 cuts out audio above 3KHz while the low end is limited only by the output coupling capacitor. In most blood flow measurement the low end is attenuated around 100 Hz to eliminate signals from vessel walls (8). In this particular application the dc response is not of direct concern unless we are interested in zero flow as our fiducial point, in which case the circuit is fully capable of response at dc if direct coupling is used in the audio circuits beyond the detector. A circuit schematic and certain specifications of the MC1596G are shown in Figure 1.3-6. The circuit shown in Figure 1.3-5 has been constructed, but not yet tested.

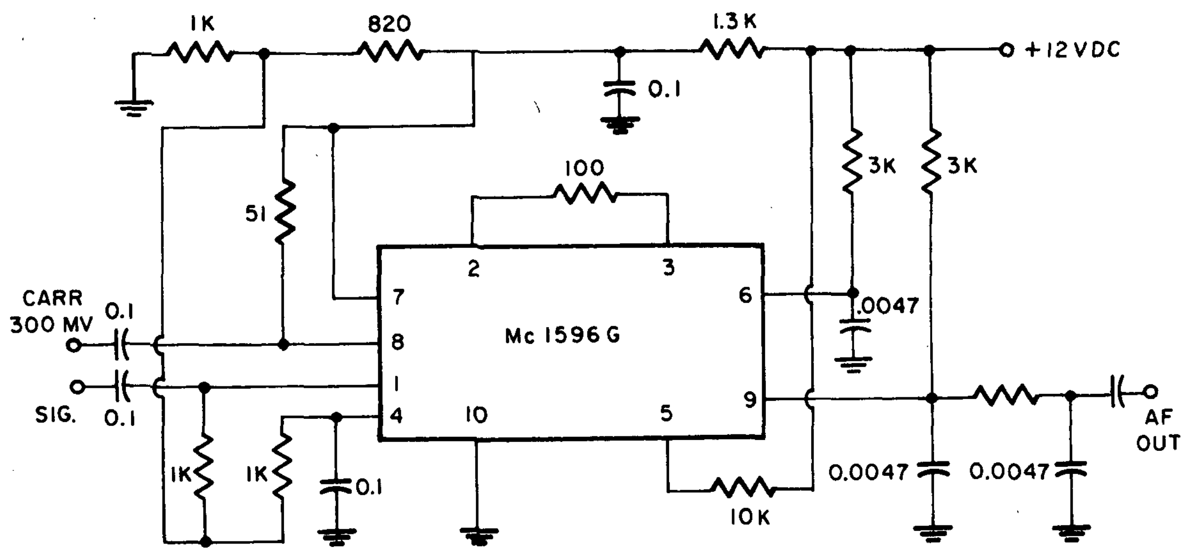

Fig. 1.3-5. Product Detector with 90 db Dynamic Range

The audio output of the detector requires amplification for further processing of the signal. This is accomplished by means of a monolithic integrated circuit, linear audio amplifier (Archer 276-016). This circuit will provide a one-watt output signal into an 8 ohm load with as low as an 8 millivolt input signal. The

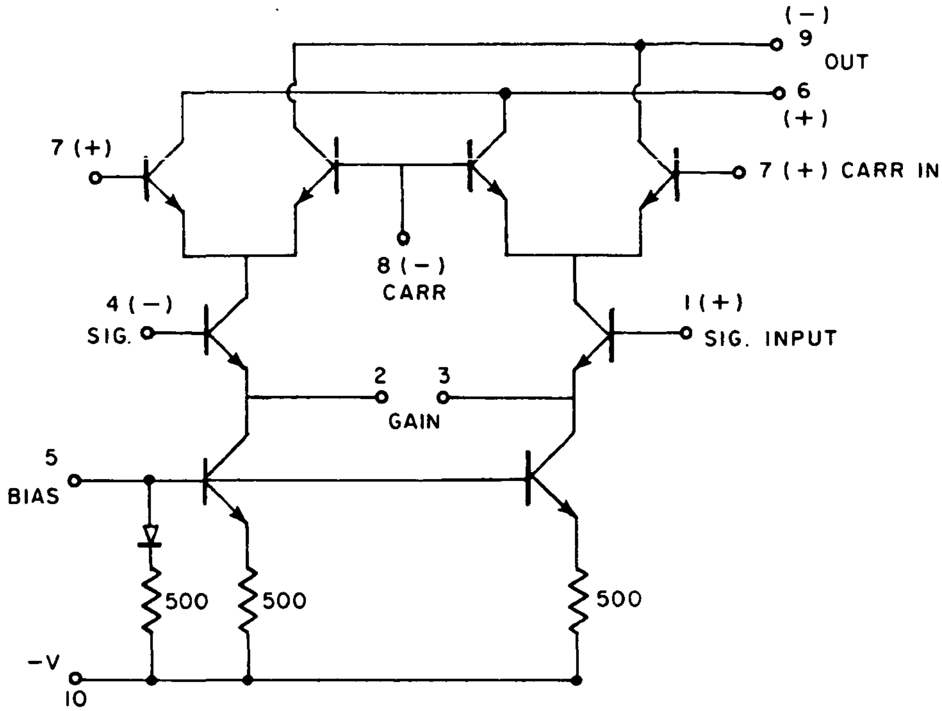

Carrier Supression - 40 db @ 10 MHz

Bal. Input & Output

Comm. Mode Rej. - 85 db

Pwr Diss @ 3 ma ≈ 33 mw

Max Pwr Diss ≈ 680 mw

Single Ended Input R ≈ 200 KΩ

Single Ended Output R ≈ 40 KΩ

Fig. 1.3-6. Circuit Schematic MC 1596G

circuit was constructed as shown in Figure 1.3-7 and tested. It performed according to specifications.

The implementation of the various components of the system has been so far, carried out according to plan. No difficulties are forseen in the design and implementation of the analog bandpass and digital bandpass filters to provide a sharp signal when flow crosses a predetermined velocity (corresponding to a predetermined frequency.)

A concise review of the various methods of measuring blood flow with some of their characteristics is given in the two tables below, Figure 1.3-8 and Figure 1.3-9. From the tables it is readily ascertained that the Electromagnetic and Doppler techniques are generally far superior to other techniques. It can also be determined that the Doppler and Electromagnetic techniques have certain characteristics which to some extent complement each other. It is on the basis of these complementary advantages that the mixed technique, Doppler-zero, Permanent Magnet flow meter is recommended. It is this mixed technique which is now under investigation and breadboard implementation.

1.4 Reference for Section 1.3

REFERENCES

(1) Annual Report A-B2299-5
Space Related Biological & Instrumentation Studies, R.J. Gibson, R.M. Goodman, March 1970 - March 1971, NSR-39-005-018.

(2) Quarterly Report Q-B2299-24, April 1971 - June 1971, R.J. Gibson, R.M. Goodman; NSR-39-005-018.

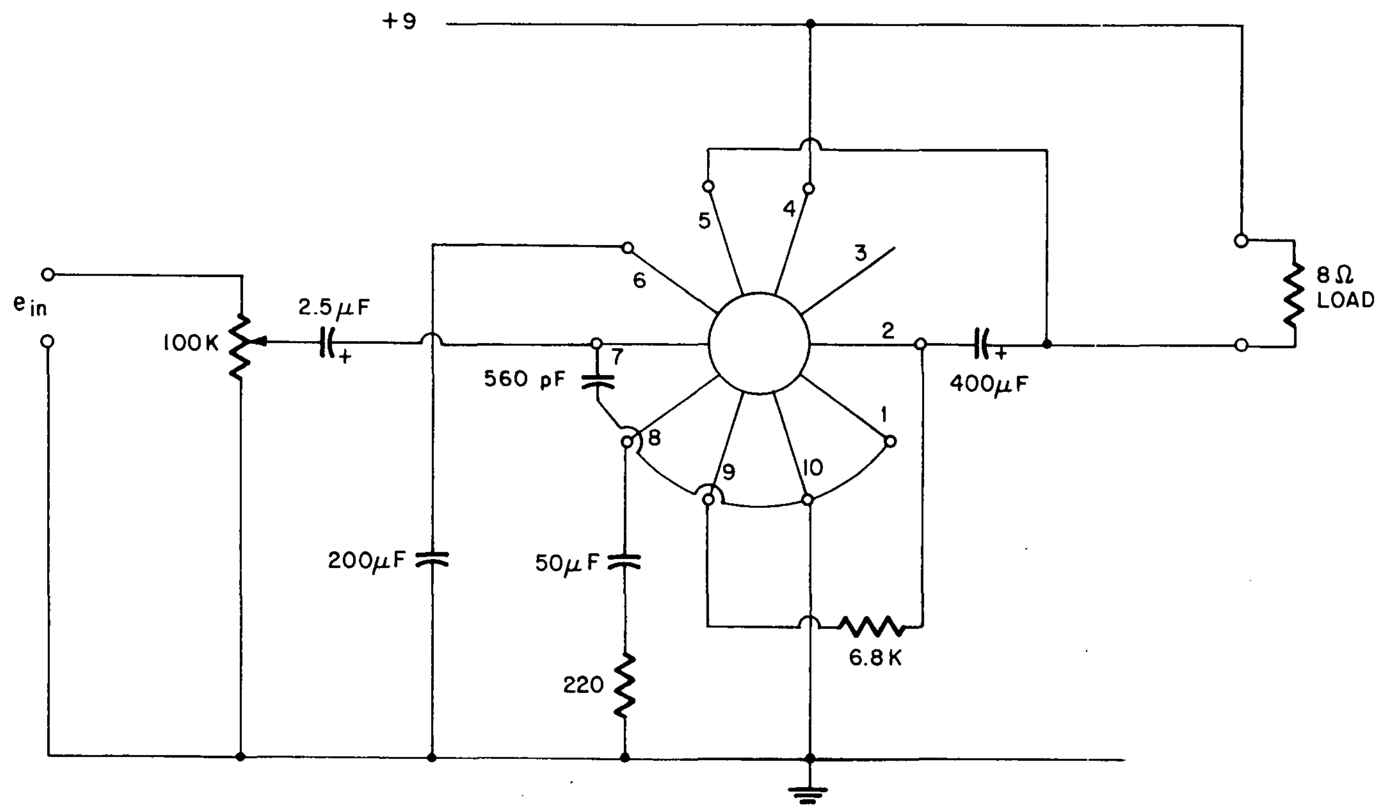

Output 1 watt into 8 ohms max.
Input 30 mv, input IMPED ≈ 10 K Ω
Distortion @ 0.5 watt, 1 KHz = 3% THD
Gain -5 db @ 50 Hz; - 2 db @ 50 KHz
Noise fig 30 Hz -15 KHz 6 db

Figure 1.3-7 Audio Output Amplifier

Method	Sub Class	Technique	Type of Flow Meas.	Meas.-Duration	Time Resolution
Electr-magnetic	Sine Wave-H Square Wave-H Constant-H	Invasive Catheter Vessel Clamp Implant	Mean volume over X-section " " " "	Chronic or Acute	Excellent Instantaneous
Doppler Ultrasonic	CW Non Dir. Directional Pulse Non dir. Directional	Transcutaneous Catheter Vessel Clamp Implant	Mean Velocity over X section Velocity at specific X-section	Chronic or Acute	Excellent Instantaneous
Transit Time Ultrasonic	Pulsed & FM	Invasive Vessel Clamp Catheter	Mean velocity over X-section " "	Chronic or Acute	Excellent Instantaneous
Differential Pressure	Pressure Gauge Differential	Invasive Catheter Vessel Puncture	Mean vol. flow X-section assumed Dist. by catheter	Acute	Good Semi-instantaneous
Thermal	Heat Pulse Thermal Cooling	Invasive Puncture Catheter	Mean col. or vel. Disturbance by Catheter	Acute	Good-Fair
Arterio-veno-gram	Radio-Opaque Fluid-Cine	Bolus injection Invasive	Mean vol. over X-section	Acute	Fair to Poor
Electron-mag. Resonance	-	Non invasive Immobilized Limb only	Mean vol. over X-section	Acute	Fair to Poor
Circulation Time	-	Tracer Dye or Radioactive Invasive	Mean volume over whole body	Acute	Poor-Time Ave.

Figure 1.3-8 Blood Flow Measurement Techniques

Flow Meter Type	Rel. Power Required	Zero Drift	Cause of Drift	Zero Check Mech	Zero Check Elec.	Flow Type	Complexity & Comment
1) Electro-Magnetic Electro-Magnet AC	Very High	Yes	Electrodes	Occlude	H-off	Volume, Aug X-sect	Hi-Gain-Heat-X sect. required Uniform H required, complex
2) Permanent Magnetic Constant-H	None for Magnet	Yes	Electrodes	Occlude	No	Volume, Aug X-sect.	Hi-Gain, X-sect. required Uniform H Required, no heat, simple
3) Doppler-non directional CW Ultrasonic	High	No	N.A.	Occlude	Yes Inherent	Velocity, aug X-sect.	Hi-gain X-sect. required Simple
4) Doppler-directional CW Ultrasonic	Twice 3)	No	N.A.	Occlude	Yes Inherent	Velocity, Aug X-sect.	Hi-gain, X-sect, required Twice comlex as 3)
5) Doppler Pulse Non directional	Lowest Doppler	No	N.A.	Occlude	Yes Inherent	Velocity, Aug X-sect.	Higher gain than 3) x-sect required About complexity of 3)
6) Doppler Pulse Directional & Ranging	Twice 5)	No	N.A.	Occlude	Yes Inherent	Velocity-specific Level of X-sect	Gain same as 5) X-sect det by ranging Twice complexity of 5) + Ranging ckts.
7) Mixed Principle PM + Doppler Zero	2) plus 5)	No	Electrode Drift Corrected	Occlude	Yes Corrected	Volume, Aug X-sect	Gain same as 2) X-sect required Complexity of 2) plus 5) plus correction ckts

NOTES:

a) A PM flowmeter alone has inherent electrode drift which if implanted cannot be determined because flow cannot be occluded nor can magnet be turned off.

b) A doppler flow meter alone has inherent zero determination but determines velocity of flow with a skewed average over a cross-section, in addition, turbulent and laminar flow produce different outputs see 8) & 10).

c) The mixed principle flowmeter is designed to eliminate the disadvantages in a) and b).

Figure 1.3-9 Comparison of Characteristics of Electromagnetic & Doppler Flowmeters

(2A) Pulsed Ultrasonic Doppler Blood-Flow Sensing, D.W. Baker, IEEE Trans. on Sonics & Ultrasonics, Vol. SU-17, No. 3, July 1970.

(3) International Ox Oscillator Data Sheet, Internation Crystal Mfg. Co. Oklahoma City, Okla.

(4) Internation PAX-1 Power Amplifier Data Sheet, See (3) above.

(5) International SAX-1 Small Signal Amplifier Data Sheet, See (3) above.

(6) Motorola Microelectronics Data Book, 2nd Ed., 1969, MC1596, Modulators & Detectors

(7) An Integrated Balanced Modulator, R. Hejhall, Ham Radio, September 1970, page 6-13.

(8) A Directional Doppler Flowmeter, F.D. McCleod, Digest 7th Conf. Med. Biol. Engineering. 1967.

(9) Technical Data, Archer 1 Watt Audio Amplifier 276-016 Radio Shack.

(10) A Doppler Ultrasound Method for Distinguishing Laminar from Turbulent Flow, B. Sigel, R.J. Gibson et. al. Jour. Sing. Res. Vol. 10, No. 5, May 1970.

2.0 THE PHOTO-OPTICAL RECORDER DEVELOPMENT

In the reporting period the recording lamphead described in a previous report (1) was completed. The mechanical design was translated into a prototype mechanical construction. We suffered some hiatus in this period caused by the death, due to illness, of our mechanical design engineer Mr. Richard Fields. Mr. Fields initial excellent start was picked up and carried forward by others on the staff.

Certain key and related circuits were constructed and evaluated.

2.1 The Recording Principle

The prototype recorder was designed to record up to thirty binary digits across a 35 mm film. This premits numbers as large as $2^{30}-1$ to be recorded.

In order to incorporate maximum versatility, we planned to operate the 30-digit recording head in such a manner that the full line of digits can be broken into a multiplicity of channels. For example, six channels of 5 bits each, or 1-channel of 10 bits, 2-channels of 7-bits and 1-channel of 6 bits, etc. This freedom permits the recording of multiple channel data and does not restrict the user to a fixed number of channels per row at all. All that as required is that the total data-group format remain constant from group-to-group.

The step-wise operation of the recorder was discussed in a previous report (ibid) and will not be repeated here. With regard to actual recording, it is sufficient to state that we plan to use Kodak film on a 2.5 mil Estar base. The emulsion used is rather similar to high speed Tri-X. Where a bit or a "1", is to be recorded, a "Pinlite" is pulsed on for ca. 10 ms.

In order to conserve funds, we incorporated the Nikon 250 exposure cassette into our recorder as film holders. The capacity of these cassettes, after slight modification of the inner diameter of the reel spools, is close to 30.5 meters (100 feet) of thin-base photographic film.

Since our planned data distribution on the film is as illustrated in figure 2.1-1, one can compute the bit capacity as follows:

$$30 \text{ bits/row} \times \frac{1}{.03 \frac{\text{in}}{\text{row}}} \times 1200 \text{ in.} = 1.2 \times 10^6 \text{ bits}$$

The limited number of recorded bits per row is caused by direct space limitations imposed by the microminiature incandescant lamps used. This limitation can be overcome by utilizing short fiber-optic links from lamps conveniently dispersed away from the film. In other words, in this latter case the lamps could be conveniently located anywhere on the recording head and their light output fed to the film through plastic or glass fibers. This more sophicated and costly approach could easily permit a data distribution as shown in Figure 2.1-2. The bit capacity

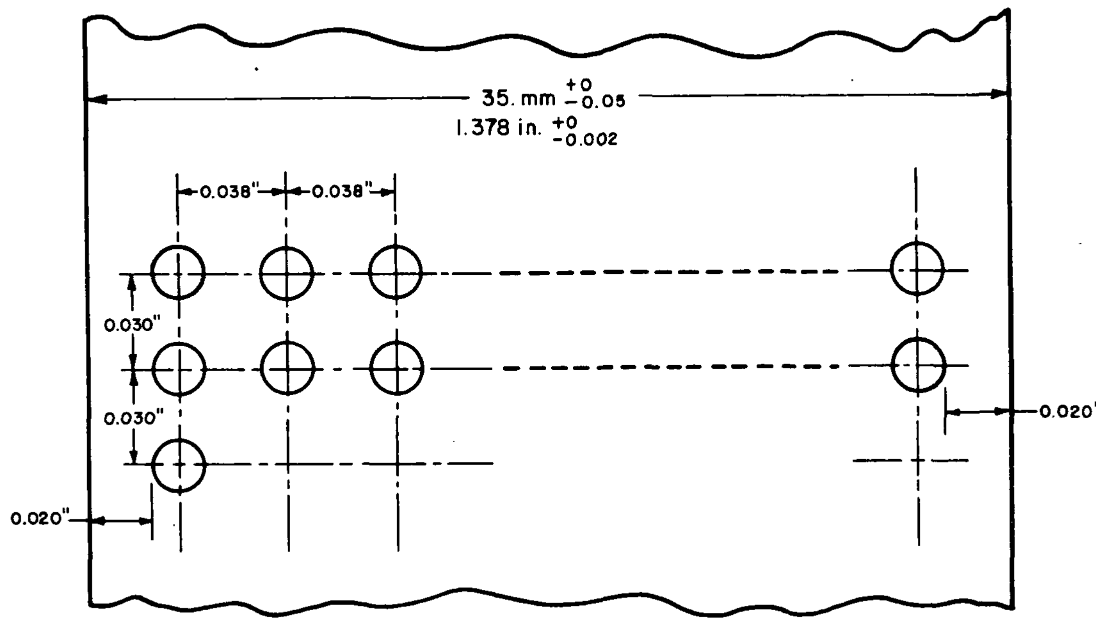

WHERE SPOT DIAM = 13.5 x 10^{-3} in.

Fig. 2.1-1. Recording Format, MK I

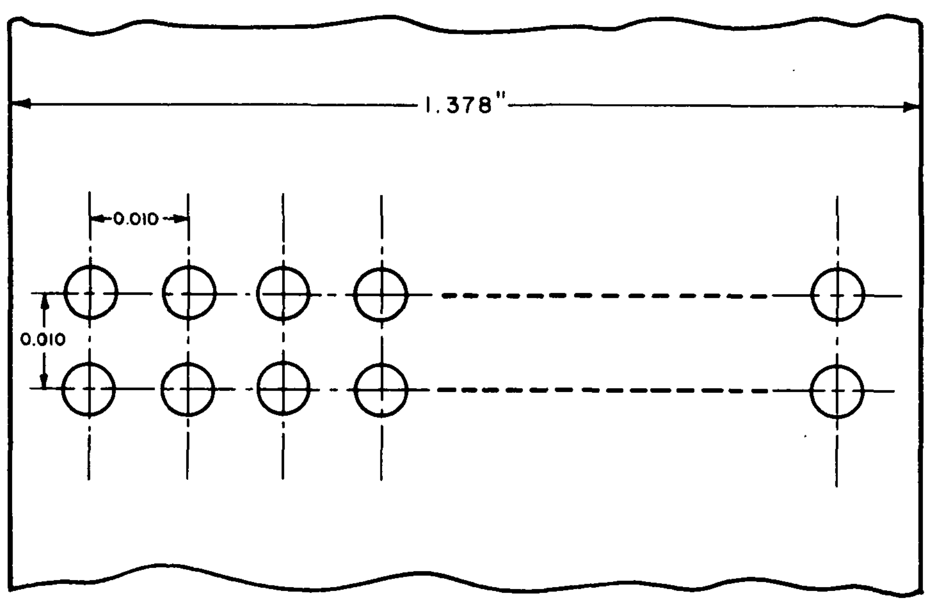

WHERE SPOT DIAM. = 5 x 10^{-3} in.

Fig. 2.1-2. Recording Format - With Fiber Optics in such an arrangement is computed as:

There are n-bits possible per row

where

$$.005\ (2\ n-1) + .04 = 1.378$$

and $n = 134$

Thus total bit capacity has become:

$$134 \frac{\text{bits}}{\text{row}} \times \frac{1}{.01 \frac{\text{in.}}{\text{row}}} \times 1200 \text{ in.} = 1.6 \times 10^{7} \text{ bits}$$

It is possible to reduce further the spot size and thus obtain even larger capacities. It seems reasonable to anticipate capacities of 2 to 4 times that calculated above.

2.2 Mechanical Design

Our approach to the prototype mechanical design was straight forward in that we wished to solve related problems of drive, etc. We planned to consider weight and size reduction as a second step. To this end, the design illustrated in Figure 2.2-1 was laid out. As noted above, the Nikon 250 exposure cassette was incorporated directly into this design.

Since we plan on using sprocketless film (to obtain improved recording density), the film is driven in a non-conventional manner. Drive is accomplished by rollers which have a cast elastomer surface. The roller material was selected for its high friction and gum strength and good resistance to abrasion. Further, it was fabricated by a casting technique which results in a close tolerence, concentric surface. Since this method requires no subsequent

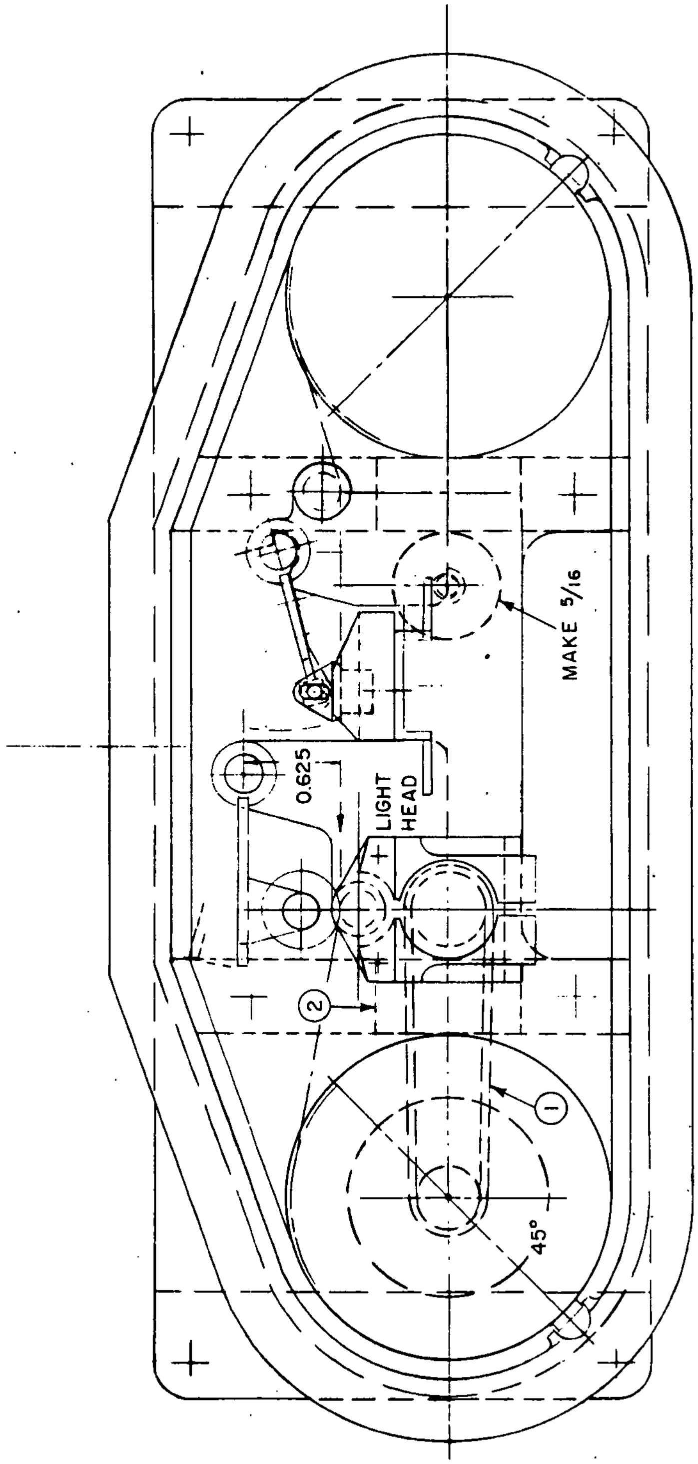

Fig. 2.2-1. MK I Recorder Design

finishing operations, no contaminating particles are embeded in the roller surface which could scratch the film. Roller drive friction is sufficient to pull the film out of the reservoir cassette and past the recording lamp head. Positive film take-up is ensured by maintaining tension through a single spring belt drive to the take-up cassette.

In the first model, ball bearings were used at all bearing surfaces.

The lamphead support assembly includes the multipin internal connector. This arrangement was so designed to permit the lamphead to be wired to the connector as an integral unit. Also, easy removal of this assembly permits the replacement of single lamps should that prove necessary.

This first prototype measured ca. 21 X 7.6 X 6.7 cm and weighed 2400 gm including 30 meters of film. We consider both the size and weight excessive for our planned application.

We conducted a design review in which each recorder component was reexamined and the following questions posed:

a. can the part be eliminated?

b. how can the part be reduced in size?

c. where can material be removed without seriously affecting strength and regidity?

d. can a lighter material be substituted?

Our first review led us to the conclusion that without a change in general configuration, total weight can be reduced about 55%. A second review led us to the conclusion that a shift to 16mm, sprocketless film and the use of a fiber optic lamphead could make possible a high capacity recorder weighing reasonably less than 0.5 kg. and would additionally result in a considerable volume saving.

Figure 2.2-1 shows the results of our first analysis of recorder weight wherein redesigned weights are in a MK II prototype, 35mm recorder.

Figures 2.2-3 and 2.2-4 illustrate a possible MK II unit using 16mm film.

2.3 Recording Head

The 30-bit recording head was machined from Nylatron and its components appeared as illustrated in Figure 2.3-1.

COMPONENT	MK I (WEIGHT)	REDESIGNED WEIGHT
Basic Assembly	1071 gm	234 gm
Cover Base	393	143
Base Plate	84	64
Capstan Plate	104	92
Drive Roller Support	44	14
Photo head mtg. brkt.	25	9
Connector bracket	5	3
Idler gear	28	24
Pressure Roller	34	6
Film hold-down arm	12	4
Cassette mount	125	37
TOTALS	1925 gm	630 gm

Weight reduction: 1295 gm (55%)
Total weight of MK I: 2385 gm

Figure 2.2-2 MK I RECORDER COMPONENT WEIGHT ANALYSIS

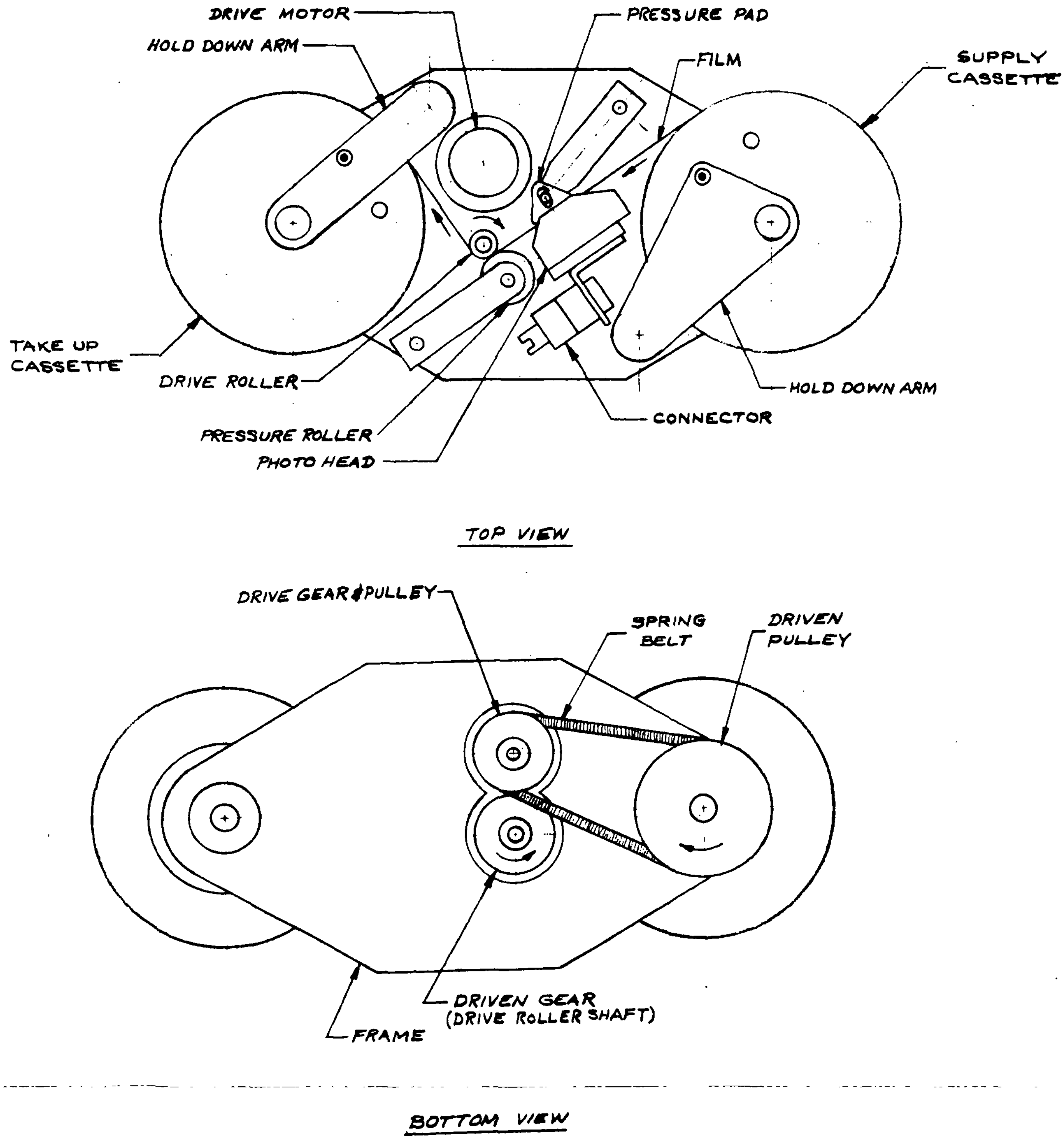

Fig. 2.2-3. A Reduced Weight and Volume 16 mm Photo Recorder

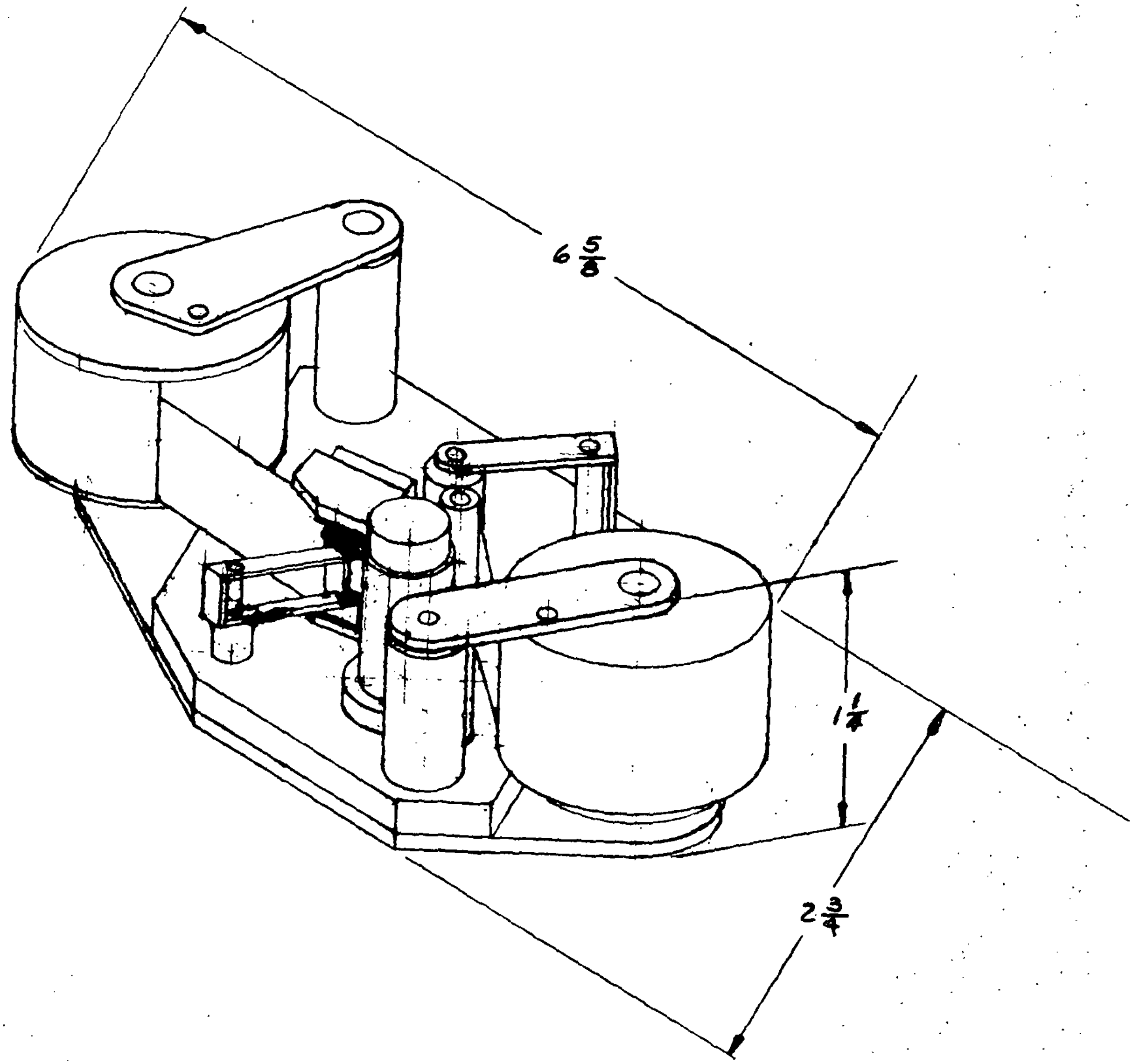

Fig. 2.2-4. Isometric of 16 mm Photo Recorder

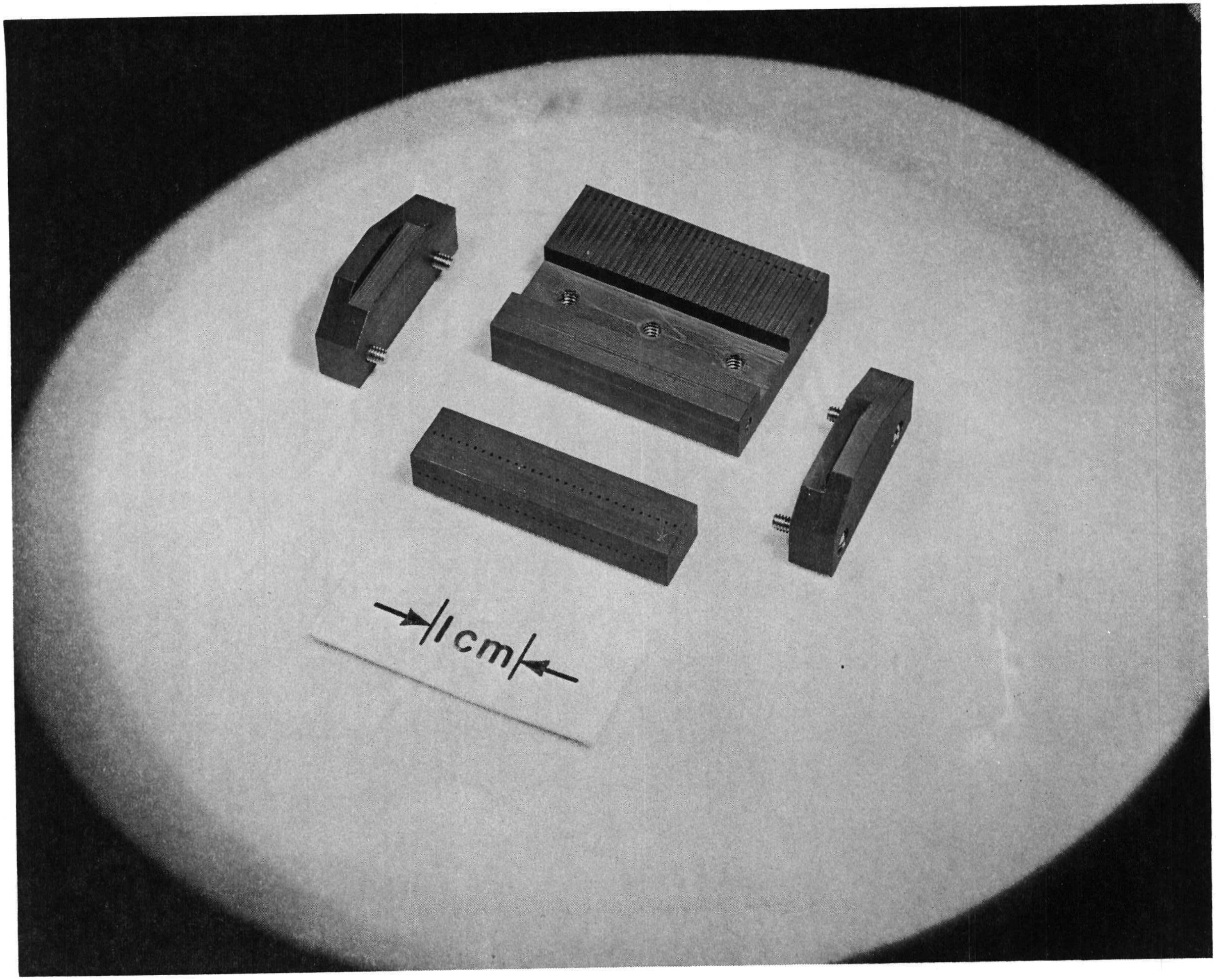

Fig. 2.3-1. Recording Head - Components

The Pinlites (type 13-7) or incandescent lamps were emplaced within the assembled head after meticulous cleaning of machining chips from all light paths. Each platinum lamp lead was pre-tinned using a stainless steel solder flux and finally the lamp leads were soldered to a common and to each of the thirty lamp busses. These "bus-bars" consisted of pure nickel strapping (.015" x .002").

The finished head appears as shown in Figure 2.3-2. After all lamps were soldered in place, each was tested with a 1.0 volt driving voltage and each finally located over the light-orifice by final adjustment of the leads. In a final model of this head we would plan to fill each light orifice with clear Sylgard 184, a clear, light transmitting silastic. A similar, but opaque material will be used to seal the lamps in place. The use of Sylgard for this purpose will make the lamphead essentially a solid assembly. The Sylgard being resilient will not stress the lamps against their leads. Further, the entire unit can be expected to be substantially shock-resistant.

The circuit designed for driving each lamp is as shown in Figure 2.3-3. Circuit performance is as follows:

QUIESCENT CURRENT DRAIN $\approx$ 0.0

e_{1-sh}	E	R	i_T	$e_\ell([e]_{\ell n}=0)$	e_ℓ	$e_{\ell n}$
2.5V	3.0V	2.2M	10.Ma.	<1MV	1.85V	.353 to .359V
2.05	2.5	2.2	6.0	<1MV	1.30V	.385 to .394
1.50	2.0	2.2	4.0	<1MV	0.80V	.412 to .419
1.25	1.75	2.2	2.8	<1MV	0.56V	.424 to .430

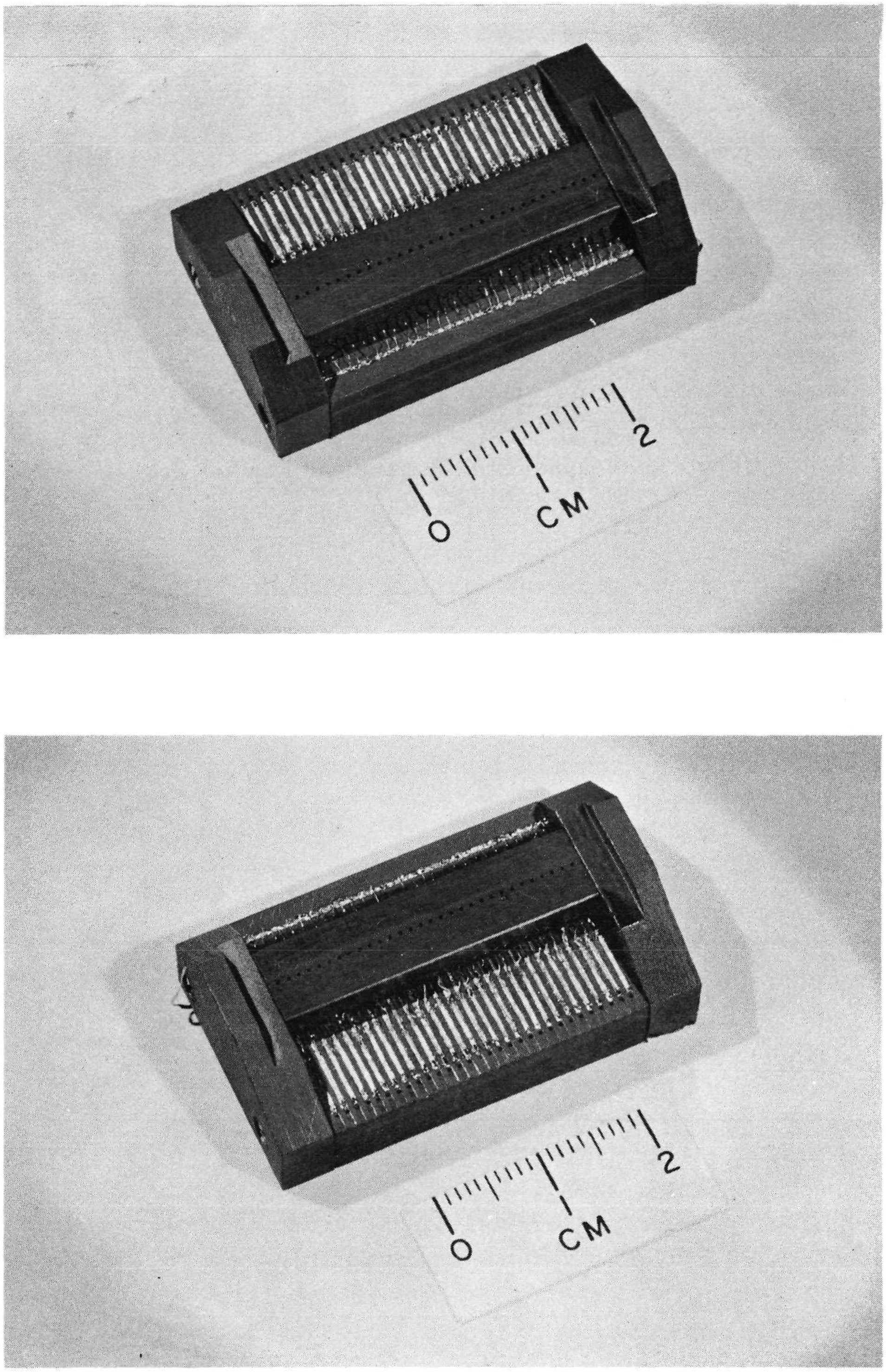

Fig. 2.3-2. Lamphead with Lamps Wired in Place

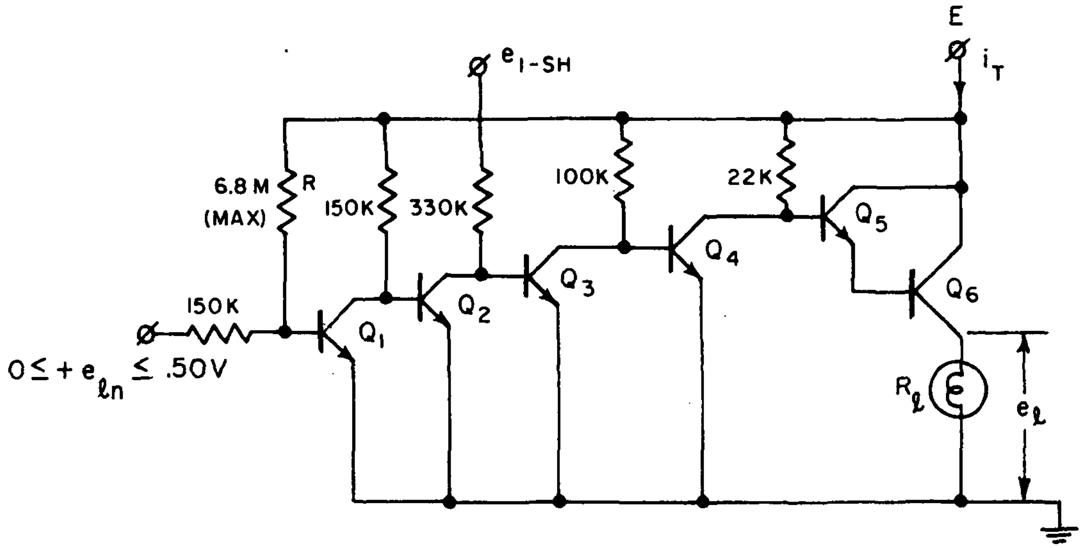

FOR ALL INDICATED MEASUREMENTS, $R_\ell = 100\Omega$ 1-SHOT $E_{cc} = E$

Q_{1-6} = LDA401 (AMPEREX)

Fig. 2.3-3. Lamp Driving Circuit

This driving circuit serves a double function: it operates as an extremely good low output-high input impedance, triple input gate with a pass-through voltage of ca. 1mv. when an input is lacking. It should be noted that all transisters are similar so that the entire circuit can easily be reduced to a very small hybrid integrated unit in the future.

Since we plan to drive the lamps with peak pulses on the order of 1.0 volt, the peak pulse power necessary is ca. 12.5mv with the average power per lamp in the low microwatt region.

The curves shown in Figure 2.3-4 illustrate the interelationships between R and $e_{\ell n}$ and E_{cc}=E and e_ℓ.

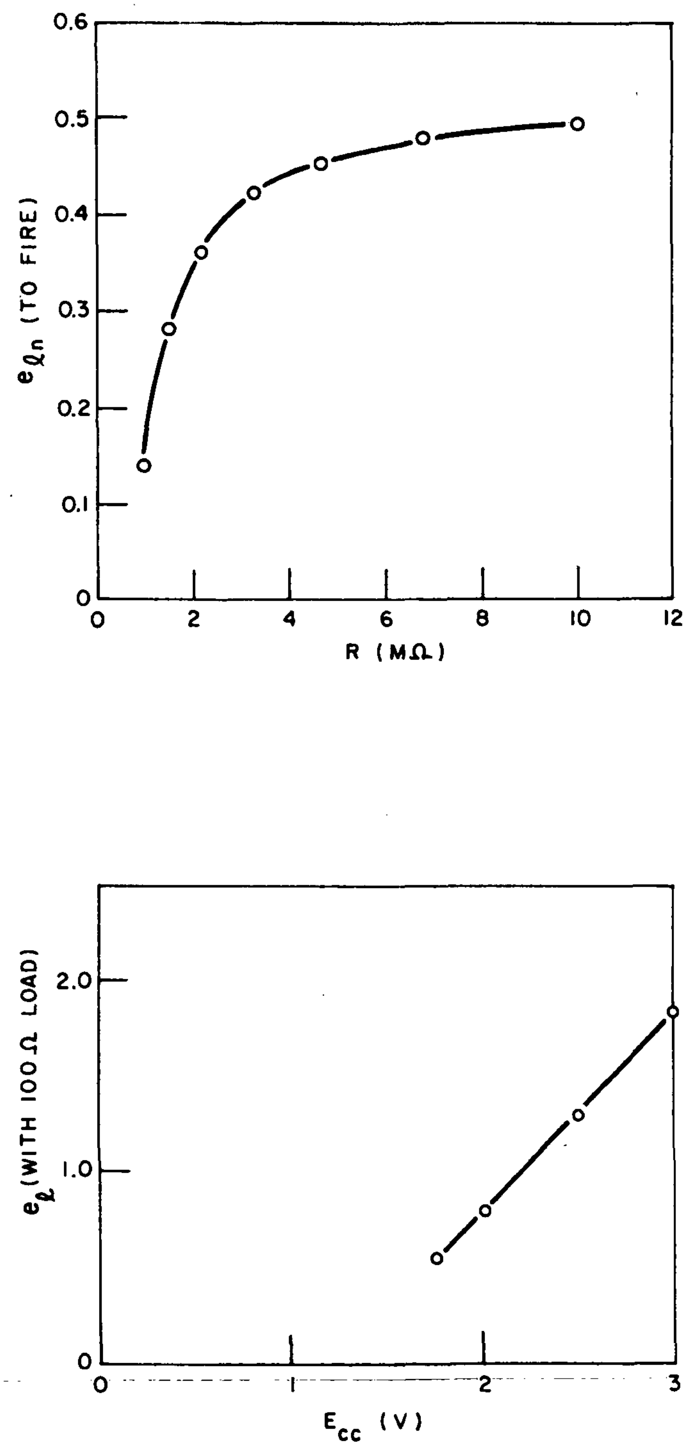

Fig. 2.3-4. Data for Lamp Driver-Gate Circuit

2.4 Drive Mechanisms

We had considered two sets of potentially useful drive motors for the recorder. The first was a fixed movement solenoid drive and the second, a microminiature dc. motor with a 5750:1 gear reduction.

The solenoid drive proved to have two potential drawbacks in this present application: it required a substantial peak current for useful operation (in view of the torque requirements) and it produced a sharp vibration and sound. The high peak current requirements occurred because we wish to operate the total system at voltage levels which necessitated a minimum of series battery arrangements. We wish to avoid unnecessary shock and vibration so that no stimili are transmitted to the animal being studied. Lastly, the efficienty of the solenoid is not high.

We determined to use a motor. The unit selected was a type 050/010 dc micromotor of Swiss design. This unit has a maximum efficiency of ca 70%. At 2 volts it is virtually free running (no load) even when driving the gear reduction. A torque load of 100 gm - cm. produced no appreciable load at the motor. The motor/gear train assembly performance was studied as illustrated in Figure 2.4-1. It was at this point that we decided to mount a tiny mirror on gear #2 of the train and to use that mirror as a control to limit motor drive for a fixed amount of film

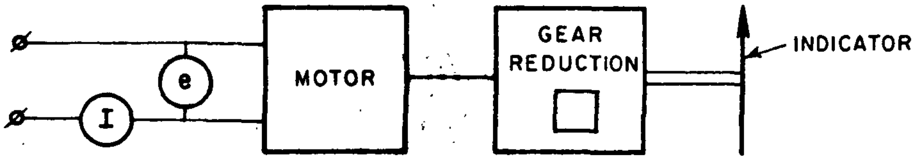

Pwr (mw)	E (V)	I (ma)	RPM Gear #2	Time for 1 rpm (Indicator)	Input RPM
14	1.00	14.	668.2	43.5 sec	7931.
19	1.25	15.	727.	40.0	8625.
26	1.50	17.	1003.	29.0	11897.
32	1.75	18.	1187.	24.5	14082.
42	2.00	21.	1353.	21.5	16047.
50	2.25	22.	1491.	19.5	17692.
63	2.50	25.	1662.	17.5	19714.
77	2.75	28.	1817.	16.0	21563.
90	3.00	30.	1939.	15.0	23000.

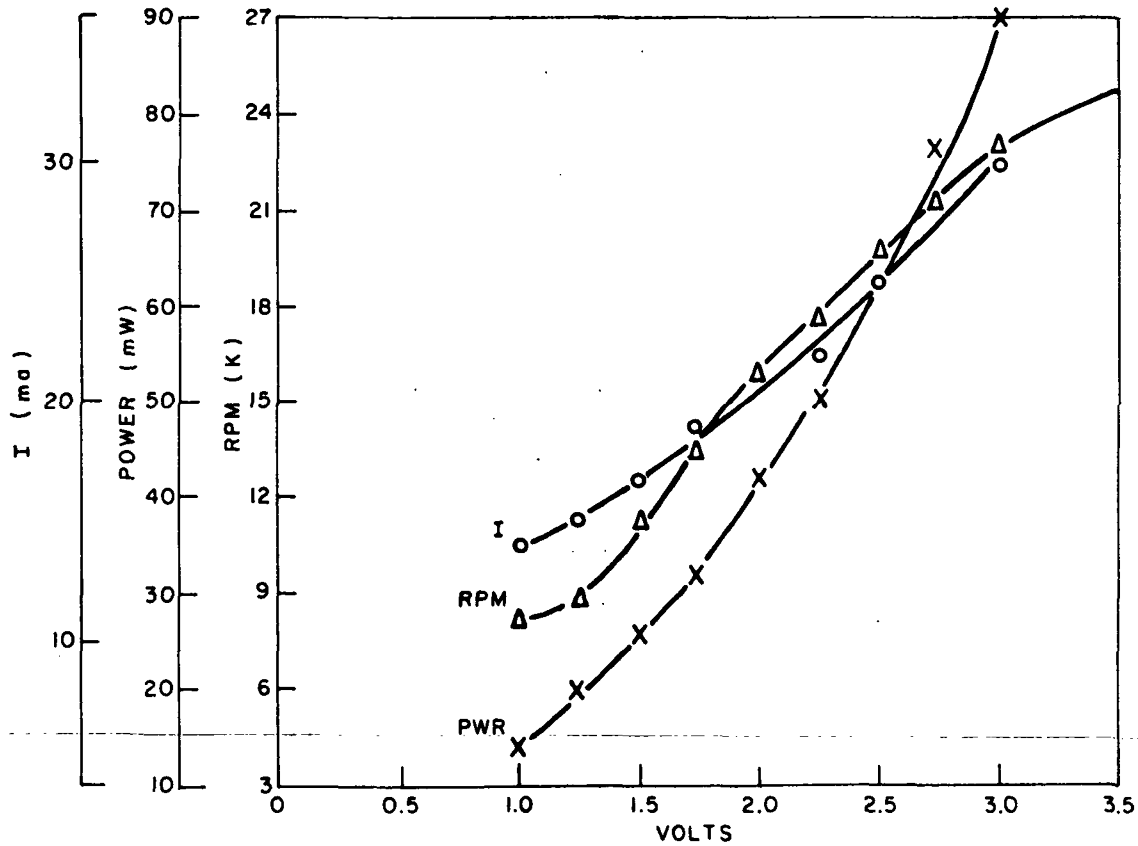

Figure 2.4-1. Motor-Gear Train Characteristics

travel. The idea behind this approach is illustrated in Figure 2.4-2. The circuits were built and tested. A tiny front-surface mirror ca. 1.5 X 1.5mm was mounted on gear #2 of the train. It was illuminated by a type 13-7, Pinlite operating at 1.0 volt. The reflected signal was picked up with a miniature cadmium-sulfide photoresistor. Circuit operation was initiated by a positive pulse input at terminal "X" on the figure. This resulted in driving the mercury relay to an "on" condition which permited the motor to run.

As the motor operated to drive the film, the tiny mirror on the 2nd gear moved around twice. Each time it permits the Binary counter to be fired. On the second time however, a carry pulse occurs at the counter; this pulse "sets" the flip-flop which closes the gate. At that point, the mercury relay automatically returns to its original condition which applies a short-circuit to the motor armature. This brakes the motor.

The entire circuit can easily be microminiaturized. It requires little power in operation. Its value lies in the fact that the 1-shot pulse originally initiated by the "X" input, does not control the motor travel, rather that is determined by the rotation of gear #2 in the reduction train.

F-B2299

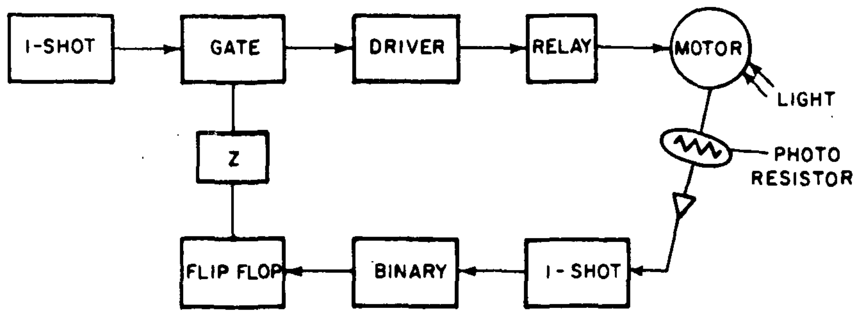

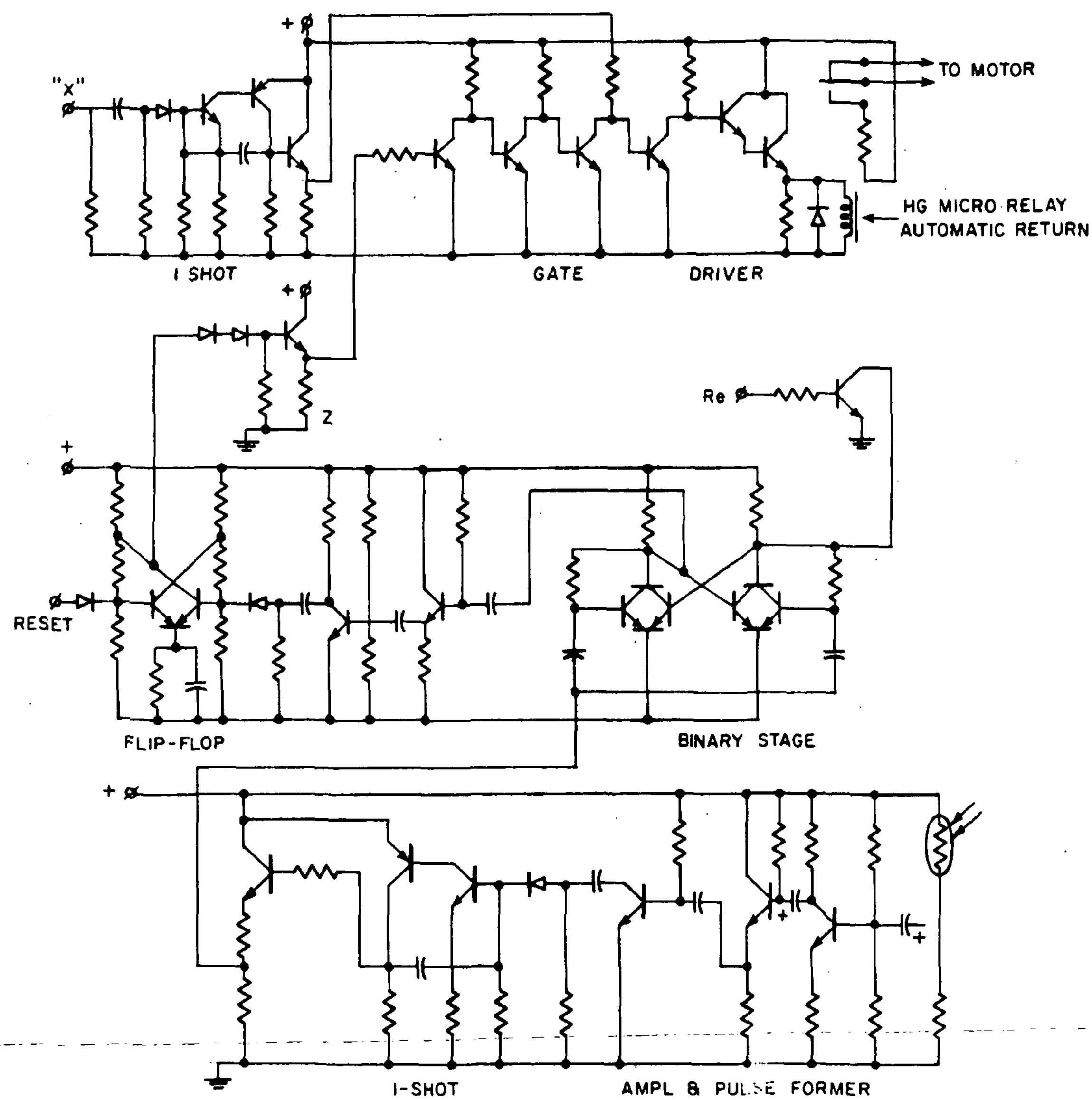

Fig. 2.4-2. Motor Control Circuit

The one-shot circuit, adapted from a circuit originally designed by M. Steele (2) has useful characteristics for our various purposes. Its performance as redesigned for micropower work is illustrated in Figures 2.4-3 and 2.4-4.

2.5 Special Circuits

Key to the circuits appropriate in accepting input data in the recorder is a 30-stage binary counter. It is of course, essential that the counter require a minimum of power and that it be convertible to n- counters if necessary. This latter point is based on our earlier observation that although the recorder has a 30-bit row capacity, we expect to put a number of channels of data on each row--and each row may have a different number of channels. This means that the counter design must be extremely versatile with input and output at every stage.

A schematic illustrating four complete stages is shown in Figure 2.5-1. Data in the performance is as follows:

Reset Operation:

E_{cc} (V)	e_g (V)
3.5	2.00
3.0	1.60
2.5	1.24
2.0	0.66

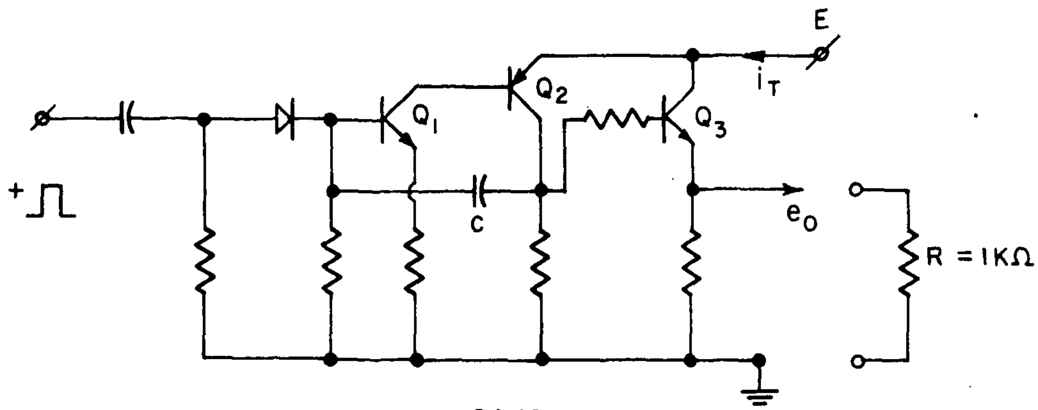

E (V)	I_T (Qursc)	I_T(pulse)	$e_o(R_L=\infty)$	$e_o(R_L=1\ K\Omega)$	PW(C = .01 μf)
3.00	0. μa	210 μa	2.50 V	2.0	10. ms
2.50	0.	170	2.05	1.6	9.5
2.00	0.	150	1.50	1.15	8.0
1.75	0.	110	1.25	0.9	7.0
1.50	0.	90	.95	0.7	6.0

Figure 2.4-3. One Shot Circuit Design

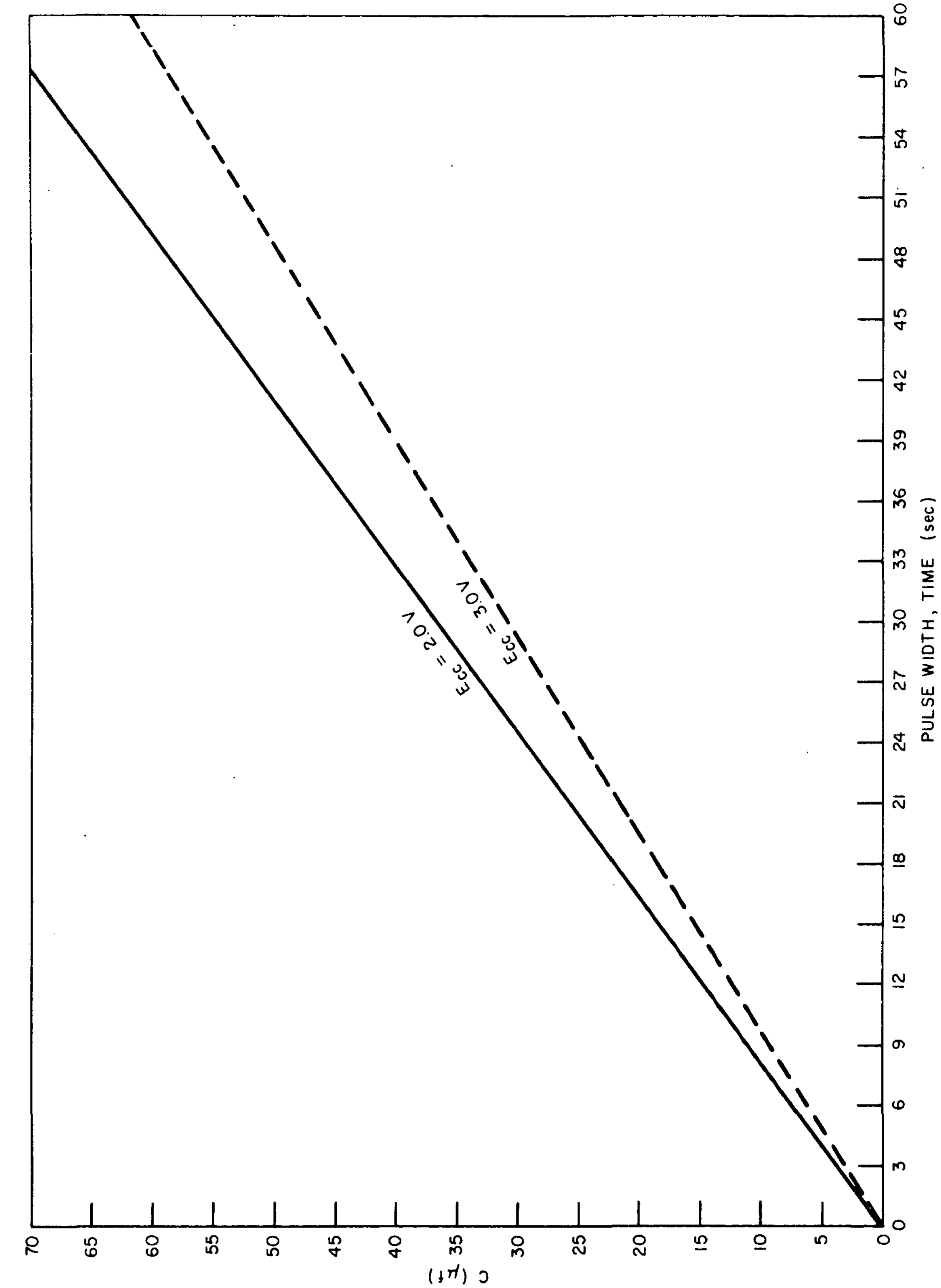

Fig. 2.4-4. One Shot Performance, T(PW) vs. C(μf)

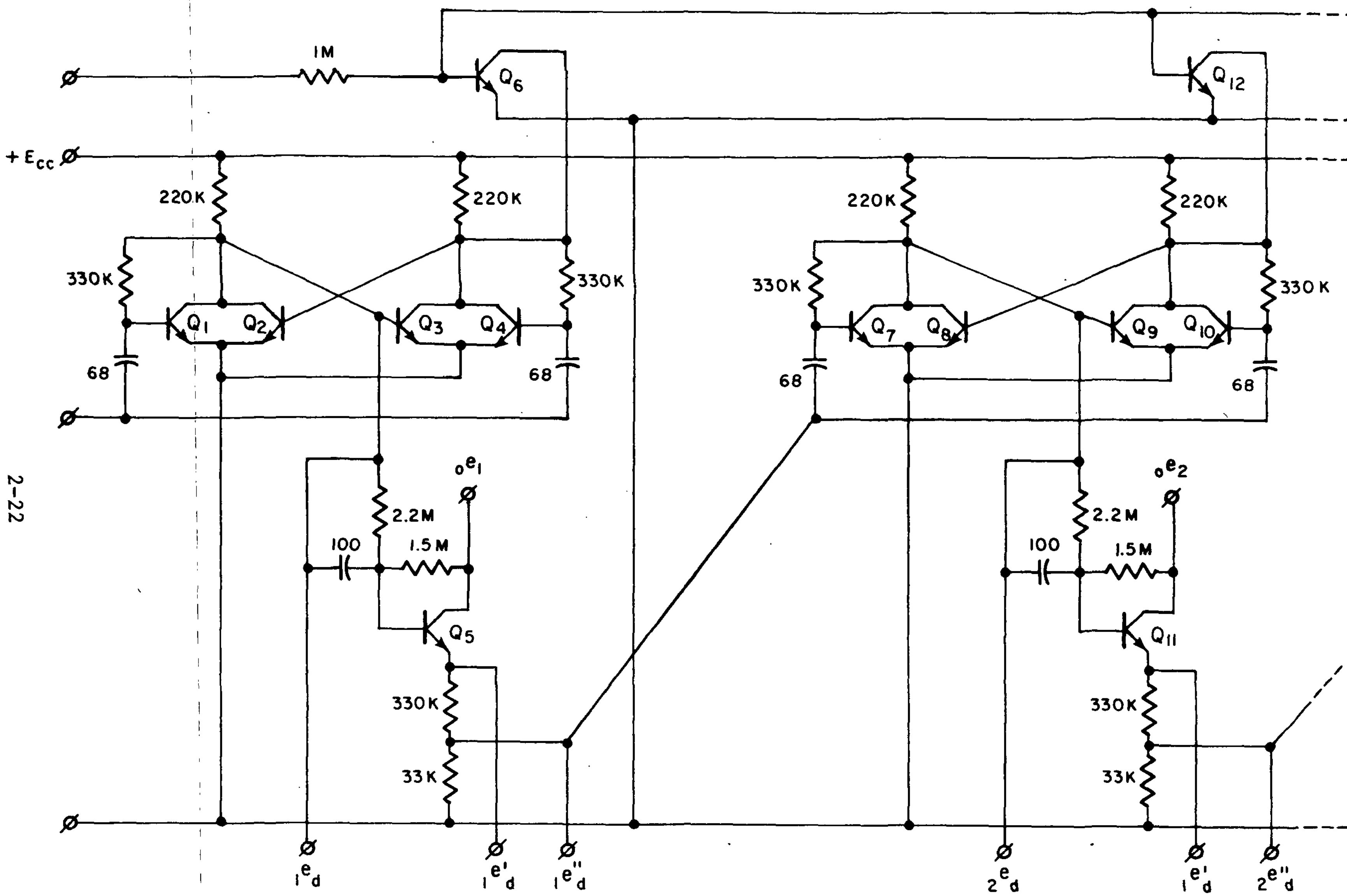

Fig. 2.5-1. Multi-Stage, Micro-Power, Controlled Binary Counter

With input e_R grounded and for $_oe_n = E_{cc}$

E_{cc} (V)	e_i $(z=1K\Omega)_{min}$	$f_{(max)}$	e_i $(z = 10K\Omega)_{min}$	$f_{(max)}$
3.5	.055	$.01 \leq f \geq 10$ KHz	0.14	$.01 \leq f \geq 50$ KHz
3.0	.060	$.01 \leq f \geq 25$ KHz	0.19	$.01 \leq f \geq 35$ KHz
2.5	.080	$.01 \leq f \geq 10$ KHz	0.25	$.01 \leq f \geq 10$ KHz
2.0	.140	$.01 \leq f \geq 8.5$ KHz	.050	$.01 \leq f \geq 10$ KHz

With input e_R grounded $e_i = 0.170V$ $(z = 1K\Omega)$ and $f = 100$ Hz

E_{cc} (V)	$_ne_d$ range for $_oe_n = 0$	$_ne_d$ range for $_oe_n = E_{cc}$	$[R_{min}$ to ground at $_ne_d]$ $(_oe_n = E_{cc})$
3.5	.02 - .52 V	.02 - .52	150 KΩ
3.0	.03 - .50	.03 - .50	220 KΩ
2.5	.05 - .50	.05 - .50	470 KΩ
2.0	.05 - .50	.05 - .50	∞

E_{cc}	I_Q $(_oe_n=0)$, f=0	I_Q $(_oe_n=E_{cc})$, f=0	I_T (f=100Hz, $_oe_n=0$)	I_T (f=100Hz, $_oe_n=E_{cc}$)
3.5	27. μa	28.5 μa	27. μa	28. μa
3.0	22.5	24.	22.5	24
2.5	18.5	19.5	18.5	20.
2.0	14.	14.5	13.5	14.5

E_{cc}	$_ne'_d$ (f=100 Hz)	$_ne''_d$ (f=1 Hz)
3.5	1.66 to 1.84	.150 to .136
3.0	1.36 - 1.53	.123 - .138
2.5	1.06 - 1.22	.096 - .111
2.0	.73 - .89	.066 - .080

Now with regard to the schematic:

$e_R \rightarrow$ Reset pulse

${}_n e_d \rightarrow$ Count pulse at exponent position n

where ${}_n e_d \rightarrow$ full output from position n

${}_n e'_d \rightarrow$ emitter follower output from position n

${}_n e''_d \rightarrow (0.1X)\ {}_n e'_d$

${}_o e_n \rightarrow$ programmed gate voltage which permits coupling between stages

In summary, the circuit levels are as follows:

$$2.4 \leq E_{cc} \leq 3.4$$

and for E_{cc} = 3.00 volts

per stage average current is:

$\bar{I}_T$ for ${}_o e_n = 0$, 23 μa

$\bar{I}_T$ for ${}_o e_n = E_{cc}$, 27.5 μa

$\therefore$ total power/stage is 69 and 82.5 μw

and

$$.037 \leq {}_1 e_d \leq .513$$

$$\Delta = .476\text{v}$$

and $0.000 \leq {}_1 e'_d \leq .014$, for ${}_o e_n = 0$

$1.36 \leq {}_1 e'_d \leq 1.53$, for ${}_o e_n = E_{cc}$, $\Delta = 0.170$v

and $0.000 \leq {}_1 e''_d \leq .0015$, for ${}_o e_n = 0$

$.123 \leq {}_1 e''_d \leq .139$, for ${}_o e_n = E_{cc}$, $\Delta = 0.169$v

2.6 The Prototype, MK I.

This effort is illustrated in photos (Figures 2.6-1 and 2.6-2. Referring to Section 2.2 above, we note that the suggested MK II unit utilizing 16mm film will substantially reduce the size and weight of the illustrated unit.

2.7 Reference for Section 2.0

(1) R. J. Gibson and R. M. Goodman, Space Related Biological and In strumentation Studies, Annual Report March 1970 - March 1971, Report A-B2299-5.

(2) M. Steele, EDN, 15 December 1969.

(3) E. Keonjian (Ed), Micropower Electronics, AGARDograph 77 Pergamin 1964.

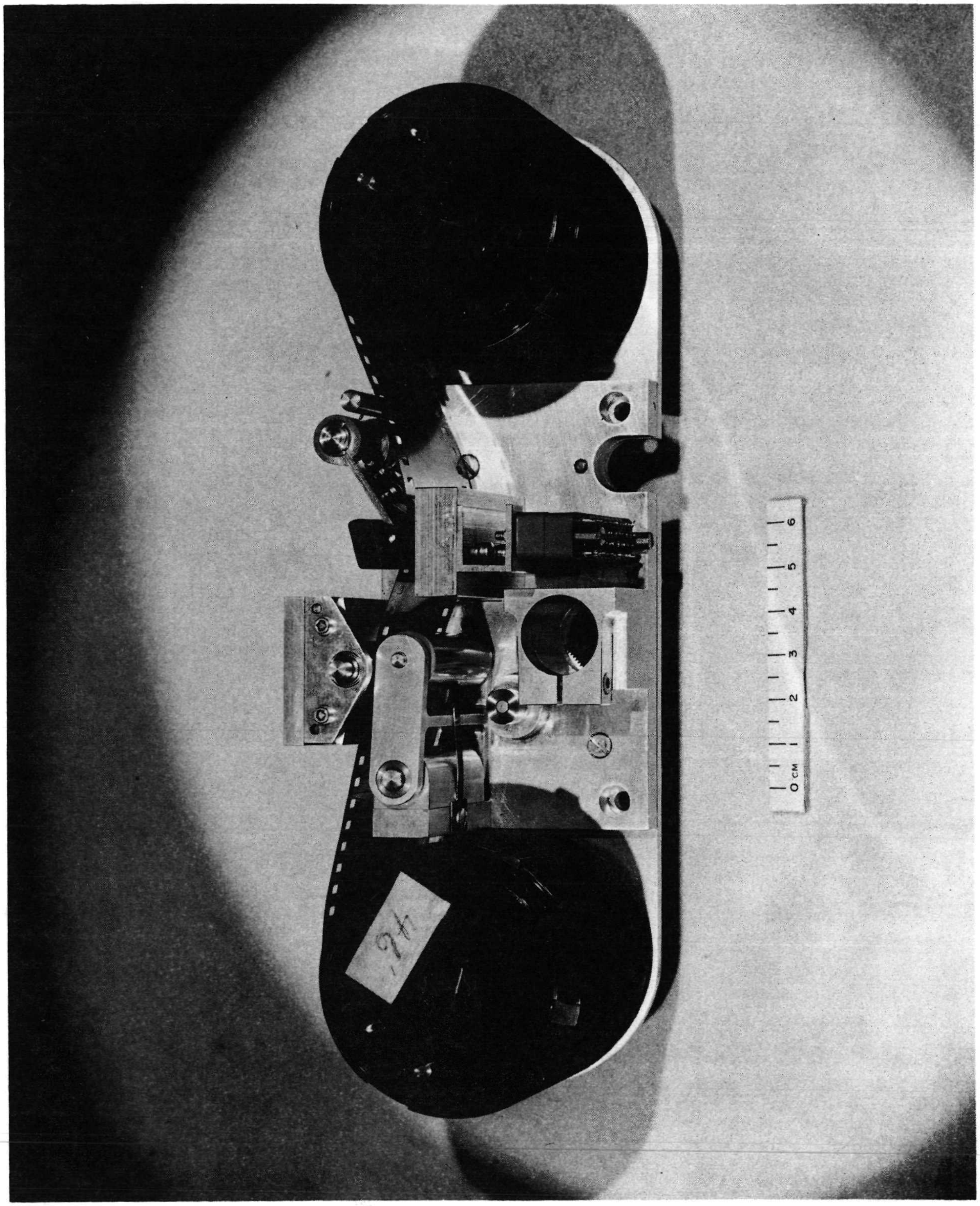

Fig. 2.6-1. MKI, Prototype Recorder

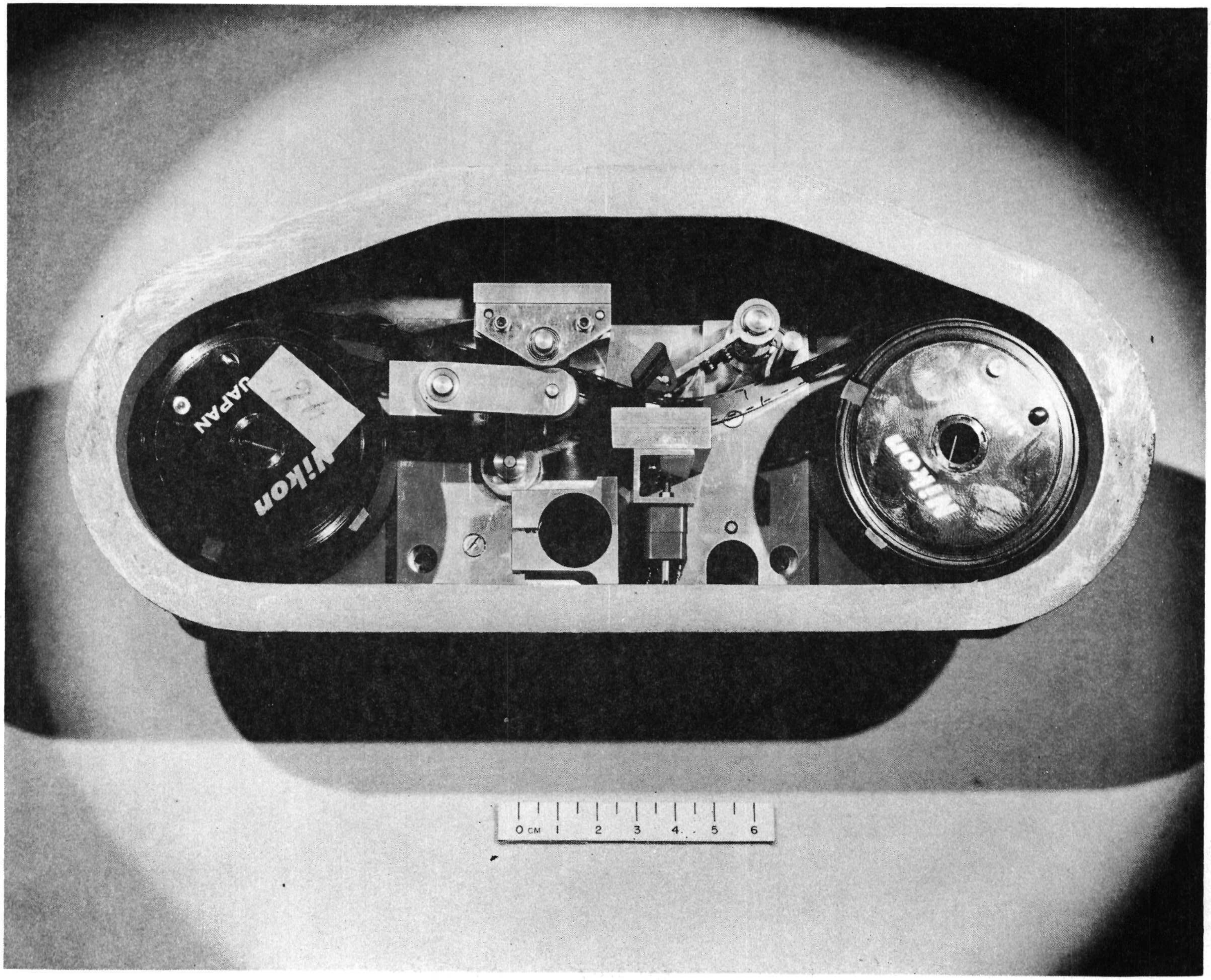

Fig. 2.6-2. MK1, Prototype Recorder

3.0 PAPERS AND COMMUNICATION

R. M. Goodman, Instrumentation for Chronobiologic Studies, presented at The Little Rock, Ark. Meeting of the Int'l Soc. In The Study of Biolo Rhythens, 8 Nov. 1971; in press.

R. M. Goodman, a Reliable and Accurate Implantable Temperature Telemeter, *BioScience* 21:8, 15 April 1971.

R. M. Goodman and R. J. Gibson, A Sealing Material for Implanted Devices, *BioScience*, 20:19, 1 Oct. 1970.

B. Sigel, R. J. Gibson, et. al, A Doppler Ultrasound Method for Distinguishing Laminar from Turbulent Flow, J. Surg. Res. 10:5, May 1970.